Tectonophysics, 50 (1978) 111—133

SUBDUCTION ZONE DIP ANGLES AND FLOW DRIVEN BY PLATE MOTION

BRADFORD H. HAGER and RICHARD J. O'CONNELL

Department of Geological Sciences, Harvard University, Cambridge, MA 02138 (U.S.A.)

(Accepted for publication April 17, 1978)

ABSTRACT

Hager, B.H. and O'Connell, R.J., 1978. Subduction zone dip angles and flow driven by plate motion. In: M.N. Toksöz (Editor), Numerical Modeling in Geodynamics. Tectonophysics, 50: 111—133.

Kinematic models of the large scale flow in the mantle accompanying the observed plate motions are calculated by neglecting thermal buoyancy forces. The large scale flow is therefore determined by the mass flux imposed by the moving plates. The energy and momentum equations decouple, and with the assumption of a radially symmetric Newtonian viscosity, the flow accompanying the plate motions can be obtained using harmonic analysis and propagator matrices. The resulting flow models predict remarkably well the observed dips of subducted slabs if the flow extends into the lower mantle. The plates drag along a thick boundary layer which should be included in models of the heating of subducted slabs.

INTRODUCTION

One very important consideration in modeling flow in the earth's mantle is that the extreme temperature dependence of effective rock viscosity, coupled with the large temperature gradient near the earth's surface, leads to the existence of a mechanical boundary layer, the lithosphere. The motion of the lithosphere implies a large-scale circulation due to the mass flux from the moving lithospheric plates themselves and viscous coupling between the plates and the underlying mantle. The motion of the plates should have a strong organizing influence upon the underlying flow, as has been shown by the experiments of Richter (1973; Richter and Parsons, 1975) and Parmentier and Turcotte (1976).

At present, numerical simulations of three-dimensional mantle convection are impractical. Complexities include the dependence of rheology on temperature, pressure, shear stress, mineralogy, and history; realistic distribution of heat sources; chemical differentiation; melting; phase changes; and the effects of the observed complex geometry. Even if realistic three-dimensional

calculations were feasible, the values of the model parameters are not well constrained for the earth. Thus, it is useful to make simpler models to investigate the effect and relative importance of complicating factors individually.

In the simple models presented here, we neglect the effect of temperature changes upon density and viscosity. This decouples the equations of motion from the energy equation and makes their solution much simpler. However, this decoupling removes the dynamics from the models. We use the observed plate motions as boundary conditions in our three-dimensional kinematic models without specifying the cause of the motion. This highly simplified model then permits us to isolate and understand the large scale flow accompanying the plates moving in their observed complex geometries.

The neglect of the buoyancy forces due to thermal and chemical heterogeneity is based on the observation that in dynamic models of convection with a moving boundary layer, the large-scale flow pattern is determined by the motion of the boundary layer even for boundary velocities as low as 3 cm/yr and Rayleigh number as great as 10^6 (Richter, 1973; Parmentier and Turcotte, 1976). Studies of the driving forces of plate motions suggest that the plates exert drag on the underlying mantle, due to concentration of buoyancy at the surface, rather than the mantle flow driving the plates as a result of distributed buoyancy (Forsyth and Uyeda, 1975; Solomon et al., 1975; Richardson et al., 1976). This is further justification for the applicability of our simple kinematic models. The neglect of the temperature dependence of the rheology is less easy to justify, but is done to make analytical modeling possible.

A major problem in evaluating numerical models of flow in the earth is that the plates themselves explain such a wide set of geophysical data that they effectively filter much of what is going on below them. However, there are some features of flow models which can be compared to observation to help assess the validity of the models. For example, the calculated normal stress at the base of the lithosphere can be compared to the observed bathymetry. Gravity anomalies can be calculated from perturbations in the radii of compositional boundaries. The shear stress at the base of the lithosphere can be calculated and compared to observations of lithospheric stress. Geochemical constraints in the form of turn-over times and segregation of source material may also be applied.

It is also possible to calculate the stress at any point in the mantle due to the flow entrained by the moving plates. That this flow pattern is dominated by the motion of the surface (Richter, 1973) indicates that the stresses in the mantle are probably not, on the average, much different in magnitude from the stresses calculated in our models. It is possible, then, to compare the computed deviatoric stress magnitudes to flow diagrams (e.g., Ashby and Verrall, 1977) to determine the probable flow mechanism. The consistency of the assumption of Newtonian viscosity can then be checked.

Mantle flow models generated using various viscosity models will be compared to these observations in another paper (Hager and O'Connell, in press).

Here we concentrate on another comparison with observation, the dip of subducted slabs.

The particle trajectories in mantle flow are observable under certain limited circumstances. In the plate tectonic model, deep earthquakes occur in slabs of subducted lithosphere. Thus the planar distributions of hypocenters in Benioff zones mark the trajectories of the subducted lithospheric slabs. The dips of the slabs, determined seismically, can be compared to the dips of the calculated velocity vectors of a flow model in order to evaluate the applicability of the model to the earth.

ANALYTIC ANALYSIS

To solve for the three-dimensional flow in the earth's mantle driven by the moving plates, we have ignored the effect of thermal buoyancy in order to calculate the large-scale flow pattern that is determined just by the mass flux imposed by the moving lithosphere. Since the Reynolds number is negligible for the earth, inertial forces can be ignored, and the viscous equations of motion have no time dependence. The models thus stimulate the flow accompanying the present-day plate motions.

The model rheology is Newtonian. Models by Parmentier et al. (1976) show that the flow pattern in some convection models is not much different for Newtonian and non-Newtonian rheologies. We also assume that viscosity is a function of radius only. This assumption may well neglect some important effects since the mantle temperature distribution is not radially symmetric, and viscosity is highly dependent upon temperature. The flow is assumed to be incompressible.

A brief summary of the mathematical method used to solve for the flow driven by the moving plates is given below. A more detailed explanation is given in the Appendix. The flow velocity and stress are expressed in terms of vector spherical harmonics. The Stokes equation can be transformed into two sets of coupled first order differential equations for each degree and order, one for poloidal and one for toroidal motions. These equations can then be solved analytically for each degree by the propagator matrix technique (Gantmacher, 1960; Gilbert and Backus, 1966; Cathles, 1975). The boundary conditions are free slip at the core–mantle boundary and the observed horizontal plate velocities at the surface. Once the Stokes equation is solved subject to these boundary conditions, the motion is determined everywhere.

HARMONIC EXPANSION OF PLATE VELOCITIES

The relative plate velocities used were those of Solomon et al. (1975). These are the relative motions of Minster et al. (1974) with slight modification. The North and South American plates are combined into one plate, and

a Philippine plate is included, using the relative motion between Eurasia and the Philippine plates given by Fitch (1972). The relative motion between the Philippine and Pacific plates is poorly constrained due to the imprecision of the Eurasian–Philippine motion determination and due to the probability of spreading within the Philippine plate itself (Karig, 1971; Anderson, 1975). Because the Philippine plate is small, this uncertainty in its motion does not have a great effect on the global flow, but it does have important local effects.

The coefficients in the vector spherical harmonic expansion of surface velocities are given by appropriate integration over the sphere. For spheroidal coefficients, a_{slm}:

$$a_{slm} = \frac{1}{4\pi l(l+1)} \int_S \left(v_\theta \frac{\partial Y_l^m}{\partial \theta} + \frac{v\phi}{\sin\theta} \frac{\partial Y_l^m}{\partial \phi} \right) dS$$

and for toroidal coefficients, a_{tlm}:

$$a_{tlm} = \frac{1}{4\pi l(l+1)} \int_S \left(\frac{v_\theta}{\sin\theta} \frac{\partial Y_l^m}{\partial \phi} - v_\phi \frac{\partial Y_l^m}{\partial \theta} \right) dS$$

Here Y_l^m is equal to $P_l^m(\cos\theta)\begin{bmatrix}\cos m\phi \\ \sin m\phi\end{bmatrix}$ and is normalized such that its mean square value is unity. The integrals were carried out numerically, using the trapezoidal rule on a $2^\circ \times 2^\circ$ grid. Calculations were done in double precision. Coefficients were calculated through degree and order twenty.

Included in Fig. 1 is the variance of each degree in the toroidal and poloidal expansions of plate velocities plotted against degree on a log-log scale. The first degree term in the toroidal expansion is omitted, since it corresponds to the net rotation of the lithosphere and is dependent upon the absolute reference frame used. It is surprising that the toroidal terms are almost as large as the spheroidal terms, since the toroidal components of velocity have no vertical motion associated with them and would not be expected to be excited, at least to first order, by thermal convection. Perhaps the large toroidal component in surface velocity is due to the extreme nonlinear effects of the mechanical boundary layer.

A departure from the general linear trend in the power spectrum is noticeable for the degree four and five terms. It is interesting to note that marginal stability calculations (Chandrasekhar, 1961, p. 244) show that modes 3–5 should be the most unstable for a body with the relative core size that the earth has.

We have compared the coefficients of the spheroidal velocity expansion with the gravity coefficients of Gaposhkin and Lambeck (1970); Gaposhkin (1974), and GEM-8 of Wagner et al. (1977) by computing correlation coefficients for each degree. The confidence levels for accepting a linear relation between flow and gravity are far below 90% except for the degree four terms. The relation for the degree four term is significant at the 90% confi-

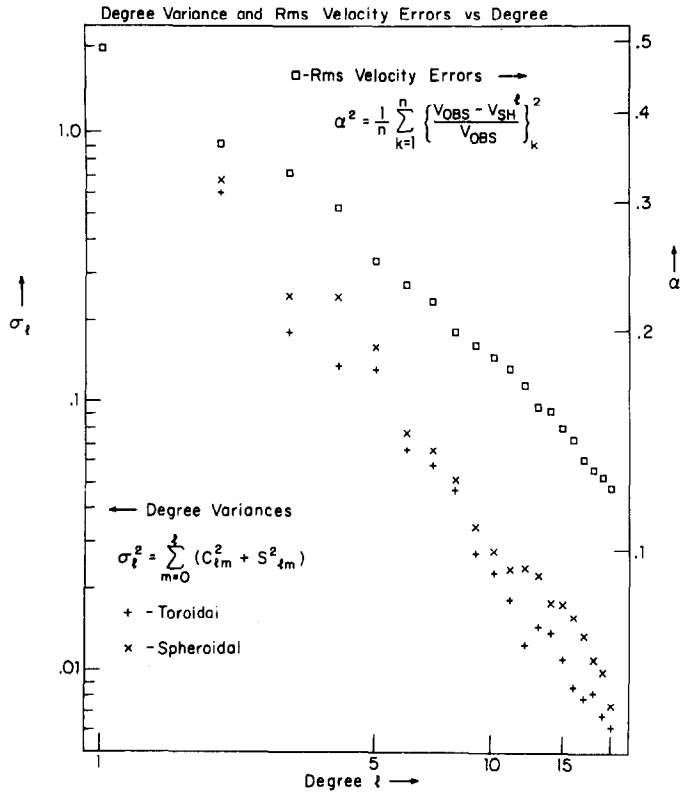

Fig. 1. Left scale: degree variance for spheroidal and toroidal terms in the spherical harmonic expansion of plate velocities plotted vs. degree. Right scale: root mean square velocity errors vs. degree.

dence level. Nevertheless, it is to be expected that, of twenty degrees tested, one degree should have this good a correlation, so the association of high power in the degree four terms with good correlation with the gravity field has no obvious significance.

Plotted on the right side of Fig. 1 is an index of the fit of the spherical harmonic expansion of plate velocities to the starting velocity model. The quantity:

$$\alpha_n = \left[\frac{1}{n}\sum_{k=1}^{n}\left(\frac{v_{OBS} - v_{SH}^{l}}{v_{OBS}}\right)^2\right]^{1/2}$$

is plotted versus degree. Here v_{SH}^{l} is the velocity at a point calculated using the spherical harmonic expansion of plate velocities through degree l. The integral is computed numerically on a $20° \times 20°$ grid. The observed velocity, v_{OBS} is taken to be in a frame in which there is no net rotation of the lithosphere. By carrying out the expansion through degree 20, we have accounted for all but about 10% of the root mean square variance in the plate velocity.

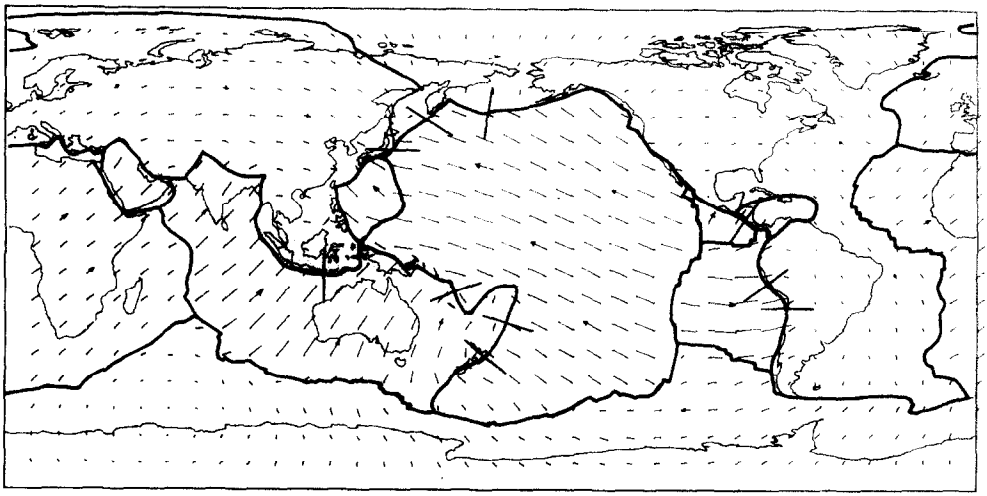

Fig. 2. Representation of the spherical harmonic expansion of plate velocities through degree 20. Relative plate motions are from Solomon et al. (1975). The absolute reference frame is that in which the lithosphere has no net rotation. Displacement vectors are plotted on a 10° × 10° grid and show the instantaneous velocity extrapolated for 10 m.y. Also shown are the locations of sections through subduction zones used in the comparison of model flow direction with seismically determined slab dip.

Figure 2 shows the results of the spherical harmonic expansion of plate velocities through degree 20 plotted on a 10° × 10° grid. The absolute reference frame is given by the condition that there be no net rotation of the lithosphere. Motions in the interior of the plates are well represented, although there are some edge effects. Even the motion of small plates, such as the Philippine and Cocos plates, is fairly well given by the spherical harmonic expansion of plate velocities through degree 20.

VISCOSITY MODELS

Although the determination of the viscosity structure of the earth is a problem in solid earth geophysics which has been studied for the past forty years, there is still disagreement as to the viscosity structure (see O'Connell, 1977, for discussion). Recent studies by Peltier and Andrews (1976) and Cathles (1975) conclude that the lower mantle has a fairly constant viscosity of 10^{22} poise. Cathles concludes that a low viscosity channel is present beneath the lithosphere, while Peltier finds the data to be better fit with no low viscosity channel.

Walcott (1973) concludes that the viscosity of the lower mantle is most likely in the range of 10^{23}–10^{26} poise, with a channel of lower viscosity above. If the viscosity of the lower mantle is on the order of 10^{25} P or

higher, the flow driven by the moving plates is confined to the upper mantle (Hager and O'Connell, in press). McKenzie and Weiss (1975) have proposed the existence of a second lithosphere at a depth of about 700 km, which would also prevent flow between the upper and lower mantle.

In this paper we have used three radially symmetric viscosity models to investigate the effect of these proposed viscosity distributions on the flow driven by the moving plates. All three have a high viscosity layer of thickness 64 km ($0.01a$) of viscosity 10^{25} P to simulate the lithosphere. This is a conservative estimate of the thickness of the lithosphere and should give a lower bound to the amplitude of the flow driven by the moving plates. The "constant" viscosity model has a constant viscosity mantle of 10^{22} P. To isolate the effect of a low viscosity channel, a model similar to that proposed by Cathles (1975) is used, which includes a channel of $4 \cdot 10^{20}$ P and thickness

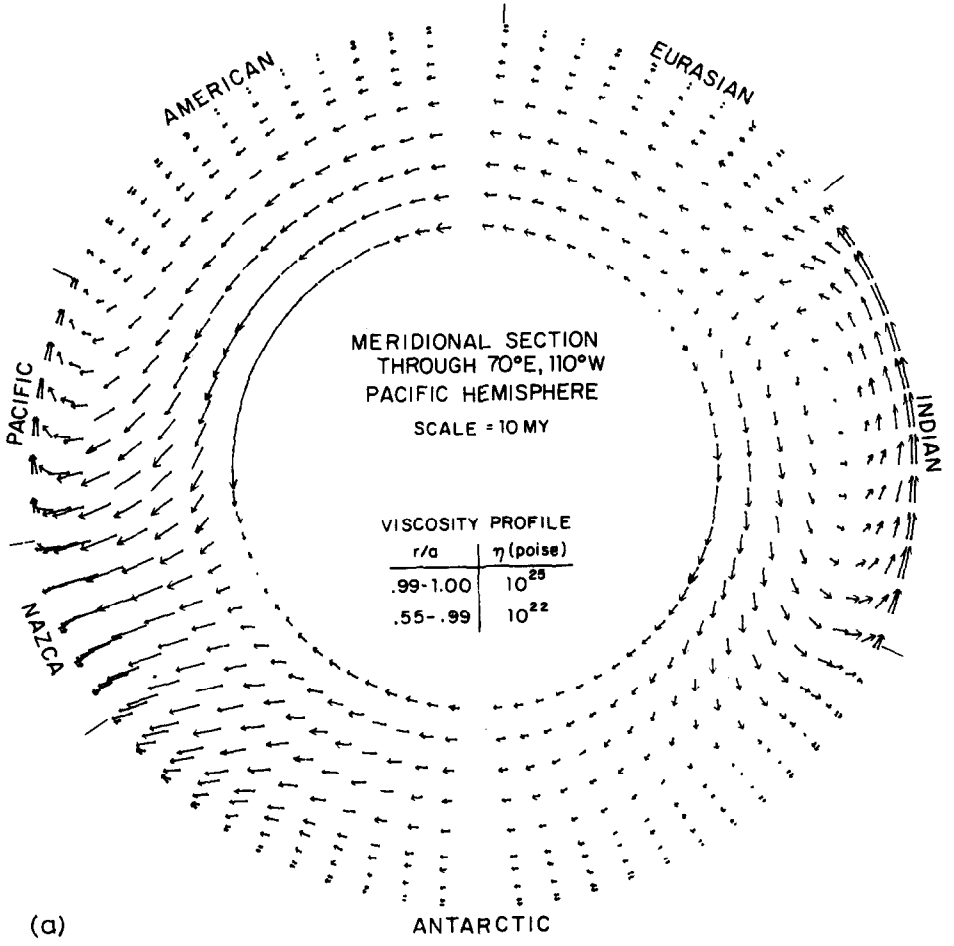

(a)

Fig. 3a. For legend see p. 119.

64 km at the base of the lithosphere in the "constant" model. A third model, the "rigid" model, constrains flow to the upper mantle by increasing the viscosity below 700 km ($r/a = 0.89$) in the "Cathles" model to 10^{25} P.

MANTLE FLOW MODELS

Figure 3 is a plot of the velocity vectors for the "constant" model for three orthogonal great-circle sections through the earth. Figure 3a shows a section through the 70°E and 110°W meridian. As can be seen from comparison with Fig. 2, the section passes through the Himalayas, near the Carlsberg Ridge, under Antarctica, across the Nazca plate close to the East Pacific rise, then on across the American and Eurasian plates. The section is viewed toward the Pacific hemisphere. The mantle flow dips beneath the Himalayas in the sense consistent with Asia overriding India.

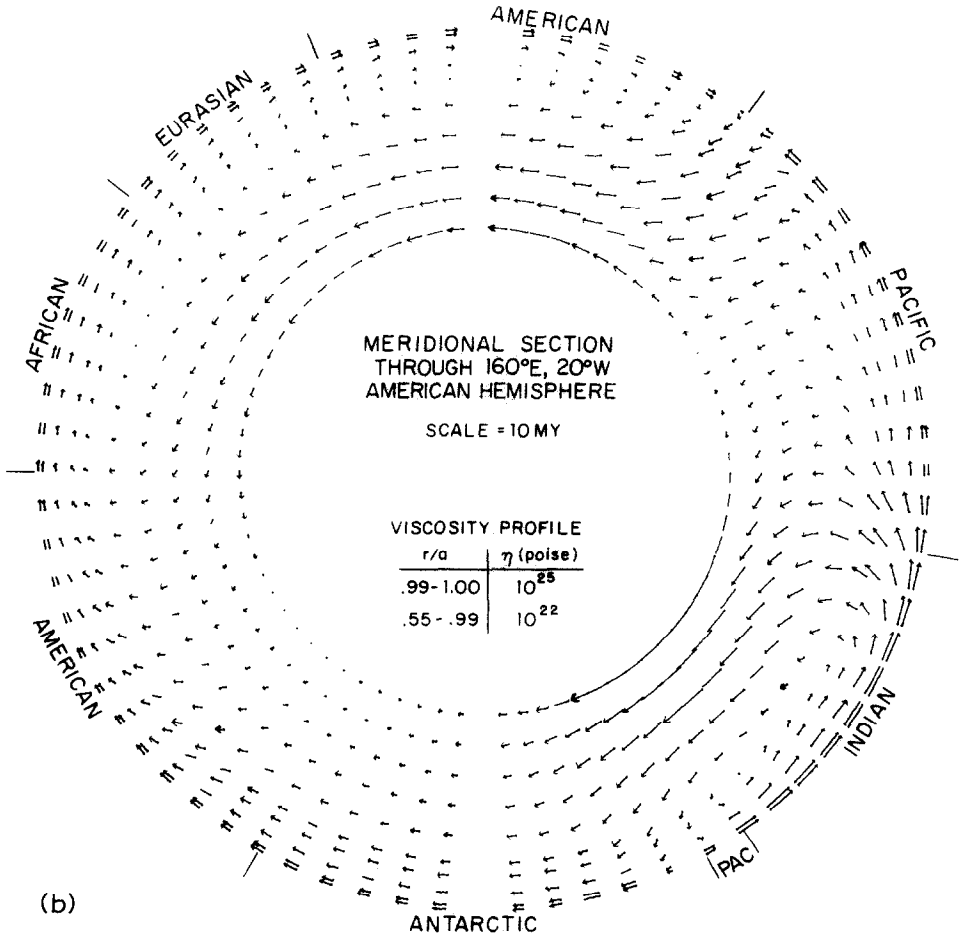

There is a strong flow from near the core—mantle boundary under the East Pacific rise and strong vertical flow under the Carlsberg Ridge.

Figure 3b is a section through 160°E, 20°W, looking at the hemisphere including the Americas. This section passes through the Kamchatka area, through the Solomon Islands and New Zealand, under Antarctica, and along parts of the Mid-Atlantic Ridge, including Iceland. The flow sense is consistent with the direction of dip of the Benioff zones under Kamchatka and the Solomons. The vertical flow beneath the Mid-Atlantic Ridge is much slower than that shown above for the East Pacific rise.

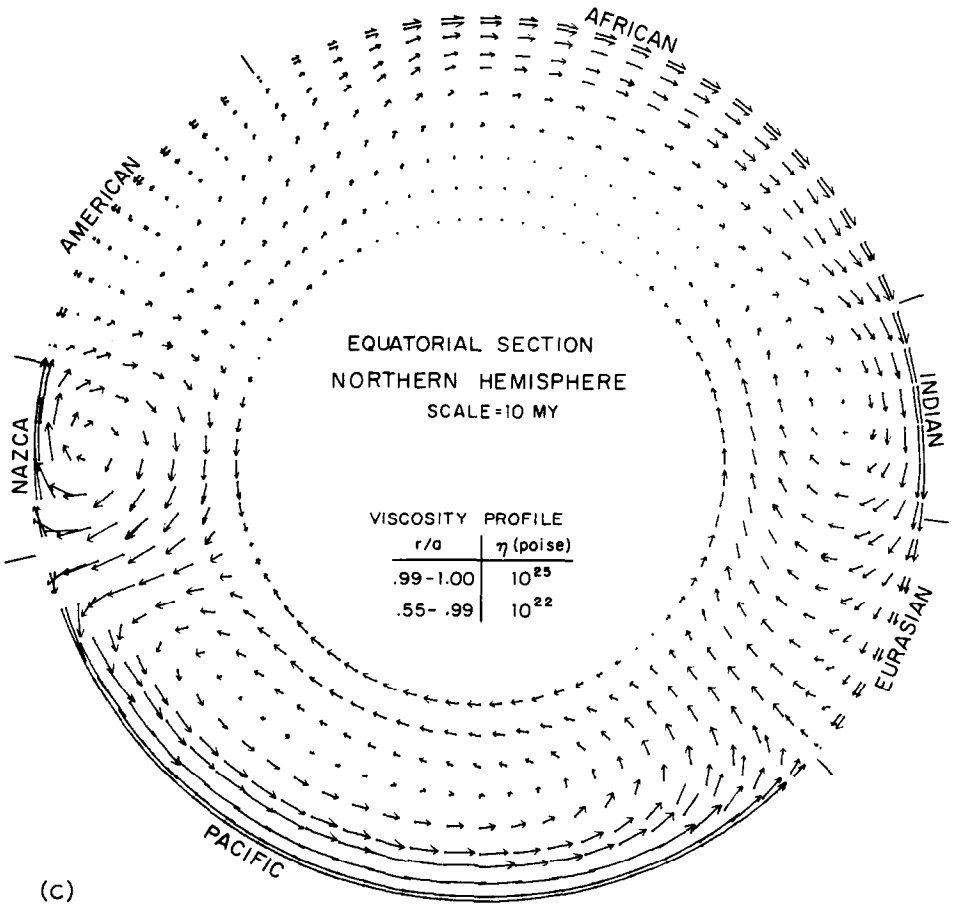

Fig. 3. Displacement vectors projected on great circle sections for the "constant" viscosity model. Displacement vectors are plotted at intervals of 5° and represent instantaneous velocities extrapolated for 10 m.y. a. Meridional section through 70°E, 110°W viewed toward the Pacific hemisphere. b. Meridional section through 160°E, 20°W viewed toward the American hemisphere. c. Equatorial section viewed toward the northern hemisphere.

Figure 3c is a section along the Equator, looking at the Northern Hemisphere. Interesting features include the consistency of the dip of the flows under Sumatra and South America with the observed direction of dip of the Benioff zones, the small cell under the Nazca plate, the strong vertical motion under the East Pacific rise, and the relative absence of shear under Africa.

SUBDUCTION ZONE DIP

Davies (1977) has suggested, on the basis of two-dimensional models of flow driven by a moving surface, that flow driven by the plates may be important in the determination of subduction zone dips. For the three great circle sections shown, the dip of the flow at convergent plate boundaries is at least qualitatively similar to the dip of the Benioff zones. One test of the usefulness of these models is to compare quantitatively the dips predicted by the flow models to the seismically determined dips.

The assumptions used in our models are weakest near the surface. The lithosphere is considered to be viscous, while an elastic-plastic rheology is probably more appropriate. Also, the truncation of the harmonic expansion at degree 20, although unimportant at depth due to the rapid decrease in amplitude of flow eigenfunctions with depth at high degree, is important near the surface. Thus we would not expect our predicted flow to be accurate in the top 100 km of the earth. In addition, it has been suggested that the dip of the upper several hundred kilometers of subducted slabs is determined by elastic effects (Isacks and Barazangi, 1977), although this conclusion might not apply in the case of very young slabs, such as those bordering Central and South America.

TABLE I

Subduction zone section parameters

Zone	Center Latitude	Center Longitude	Strike	v_0 (cm/yr)	v_s (cm/yr)	"Constant"	
						θ_{flow}	θ_c
Sunda	10°S	118°E	0°	0.78	5.88	83	76
New Zealand	40°S	178°E	135°	0.00	4.95	160	160
Tonga	26.5°S	176°W	109°	1.14	6.38	130	122
New Hebrides	16°S	166°E	70°	5.17	4.46	91	41
Japan	37°N	142°E	90°	1.96	7.53	121	107
Kurile	48°N	156°E	125°	0.61	6.54	126	121
Aleutian	51°N	179°E	3°	1.37	2.33	67	43
Middle America	11°N	88°W	45°	0.53	10.09	28	27
Peru	12°S	79°W	60°	0.40	9.31	22	21
Chile	21.5°S	71.3°W	89°	0.29	9.26	29	29

With these arguments in mind, we have restricted our comparisons to areas where old lithosphere reaches a depth greater than 200—300 km. With the exception of an ill-defined zone in the Calabrian area near Sicily, the seismic zones meeting these criteria are on the margins of the Indian and Pacific Oceans (Isacks and Molnar, 1971). We were able to obtain from the literature sections of the seismicity through the convergent boundaries of the Indian, Pacific, Cocos, and Nazca plates at approximately equal intervals. The locations of the sections used in comparison with flow dips are shown in Fig. 2. Information on the sources of hypocenter locations for these sections is given in Table I. Sections involving the Philippine plate were not used because the relative motion between the Philippine plate and the Eurasian and Pacific plates is very poorly constrained.

Figures 4a—j are plots of the hypocenter locations for the ten sections shown in Fig. 2 superimposed on the flow pattern predicted by the three viscosity models. In each figure, the top section is for the viscosity model with constant mantle viscosity of 10^{22} poise below the 10^{25} poise "lithosphere". The middle section is for the "Cathles" viscosity model. The bottom section is for the model which has an effectively rigid lower mantle, confining flow to the upper mantle. Flow vectors are plotted at intervals of 2.5°. The upper 700 km of the earth is shown in each section.

The match between the direction of flow and the direction of the subducted slab given by the trend in hypocenters is fairly good for the "constant" model for most of the subduction zones. The match is usually improved by the inclusion of a low viscosity layer in the "Cathles" model. For the "rigid" viscosity model, the flow driven by the moving plates is often in a direction counter to that observed for the subducted slabs.

To test the hypothesis that the dip of the slab is determined by the flow

"Cathles"		"Rigid"			Source
θ_{flow}	θ_c	θ_{flow}	θ_c	$\theta_{seismic}$	
113	106	166	163	72	Fitch and Molnar (1970)
109	109	13	13	109	Ansell and Smith (1975)
130	121	11	10	131	Cohn (1975)
83	40	31	14	64	Isacks and Molnar (1971)
143	132	132	119	155	Cohn (1975)
141	138	148	145	132	Cohn (1975)
32	20	38	24	60	Engdahl (1973)
86	83	150	148	69	Dewey and Algermissen (1974)
19	18	82	79	4	Barazangi and Isacks (1976)
22	21	25	25	38	Barazangi and Isacks (1976)

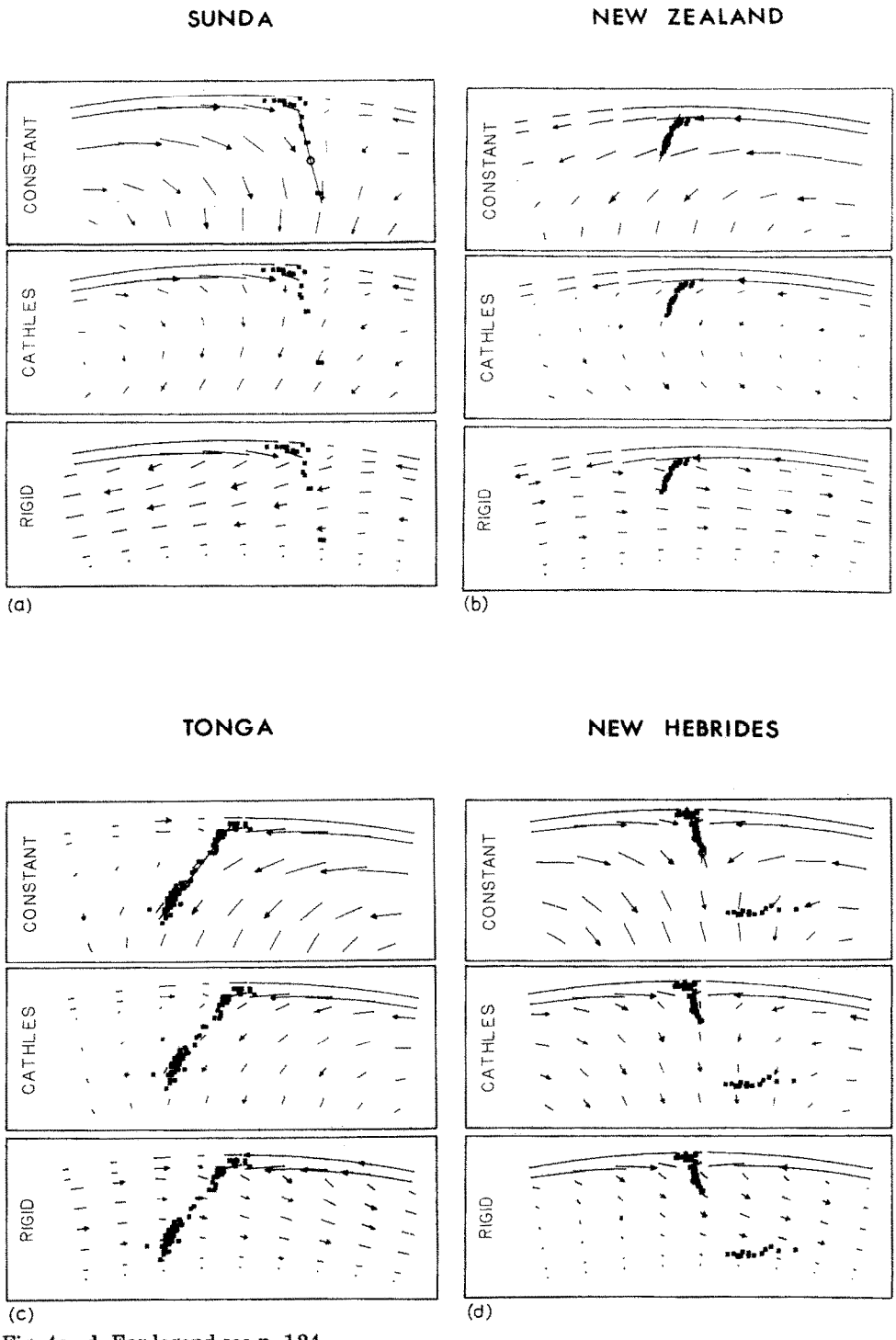

Fig. 4a—d. For legend see p. 124.

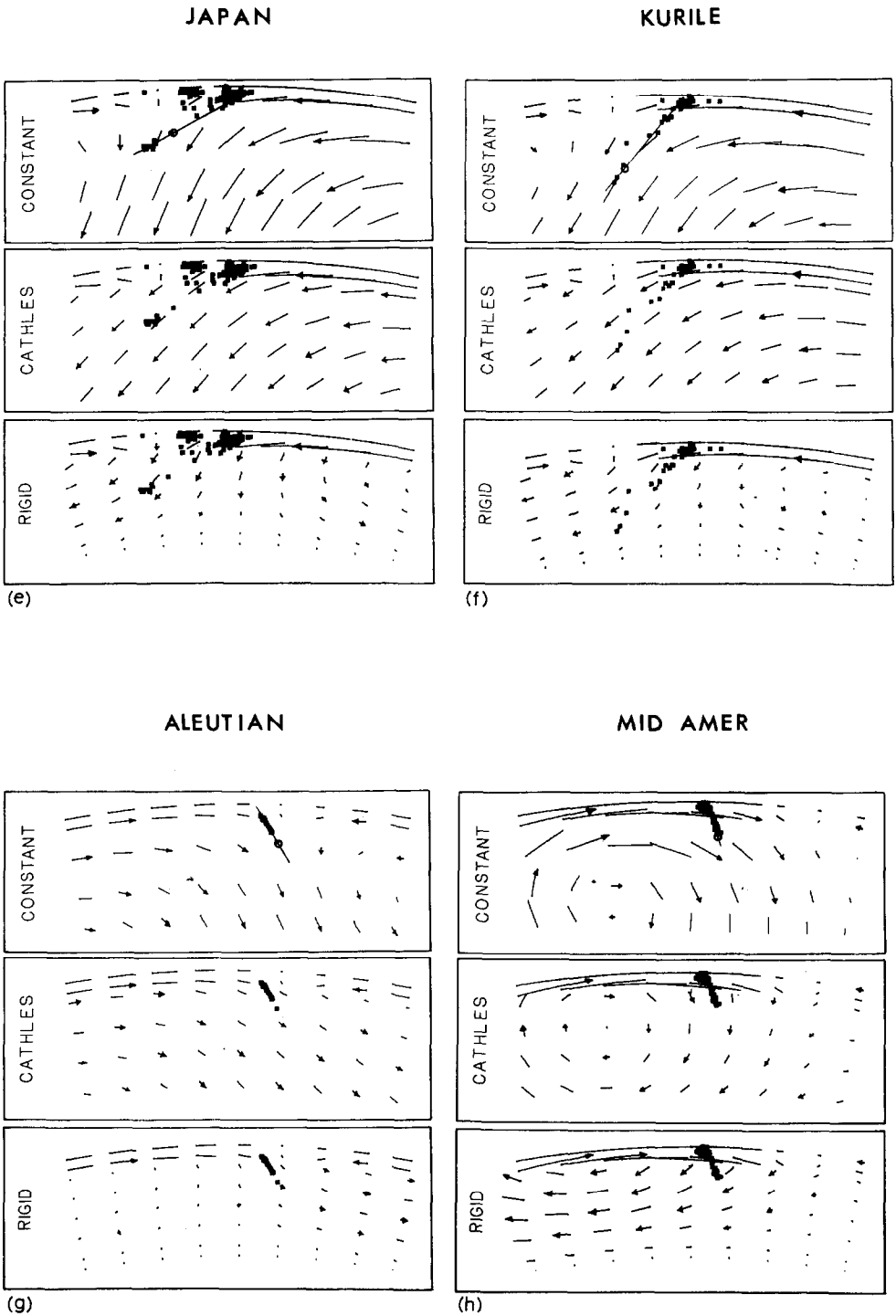

Fig. 4e—h. For legend see p. 124.

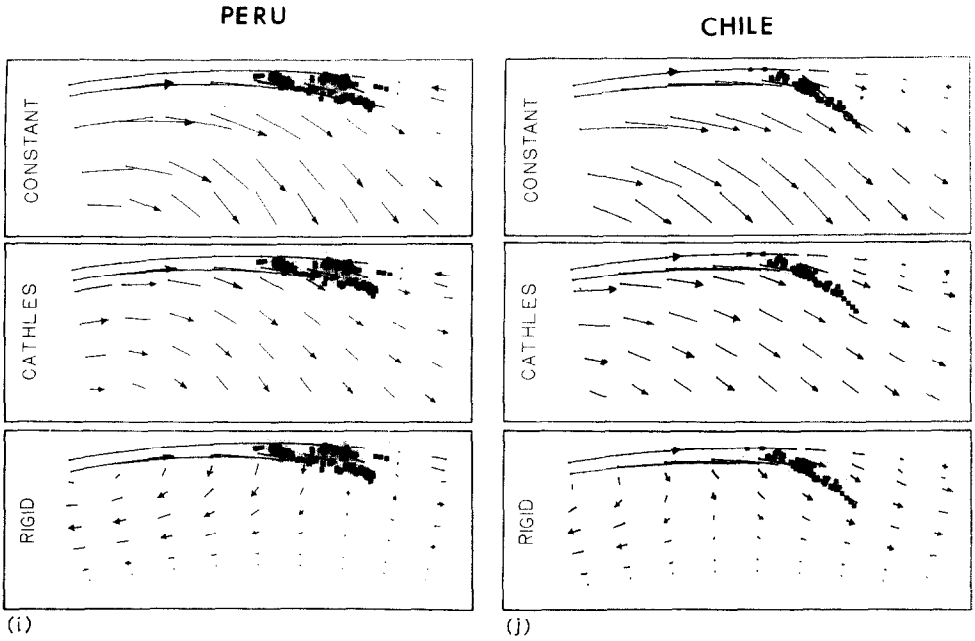

Fig. 4. Flow vectors and earthquake hypocenters projected on sections through the subduction zones shown in Fig. 2. Flow vectors are instantaneous velocities extrapolated for 7 m.y. and are plotted at an interval of 2.5° in the upper 700 km of the earth.

pattern, we have measured a dip for each seismic zone and an average dip for the flow pattern, and calculated a linear regression. The dip assigned each seismic zone is shown by the solid lines in Figs. 4a—j. The average flow dip at the point circled was calculated by linear interpolation of the four adjacent points where the flow vector was plotted. For each viscosity model, we calculated the correlation coefficient:

$$r = \frac{\sum_{i=1}^{10} (x_i - \bar{x})(y_i - \bar{y})}{(\sum (x_i - \bar{x})^2 \sum (y_i - \bar{y})^2)^{1/2}}$$

and the least squares slope m and intercept b in the relation:

$$y = mx + b$$

where y_i is the flow dip and x_i is the seismic zone dip of one of the ten subduction zone sections used. The significance of the correlation coefficient r is found by calculating "Student's" parameter $t = r[(n-2)/(1-r^2]^{1/2}$ for $n = 10$, and comparing it to a one-sided Student's distribution with $n-2$ degrees of freedom (Cramer, 1946). The results of the regression are shown in Fig. 5.

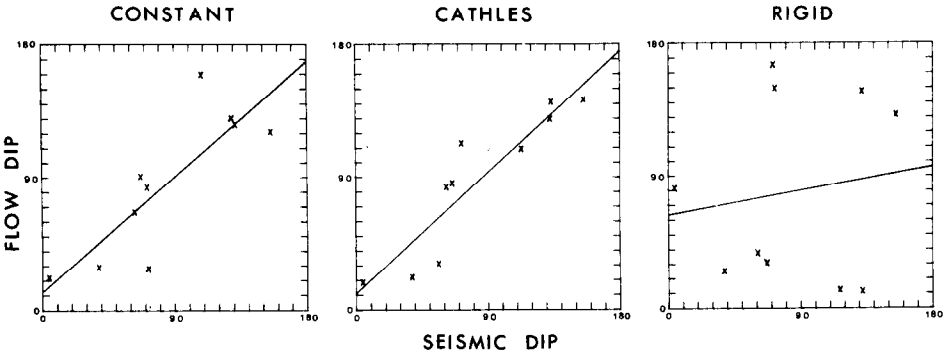

Fig. 5. Plots of the dip of the flow vs. the dip of the seismic zone for the subduction zones and viscosity models of Fig. 4.

For the "constant" viscosity model, the correlation coefficient $r = 0.83$ is significant to a confidence level of greater than 99%. For the "Cathles" model, the inclusion of the low viscosity zone improves the correlation coefficient to $r = 0.91$ which is significant at the 99.9% confidence level. The correlation breaks down when flow is confined to the upper mantle in the "rigid" model where $r = 0.14$, which can be considered to be significant at a confidence level of only 65%.

It has been suggested on the basis of shock wave data and velocity-density systematics that the lower mantle is enriched in iron with respect to the upper mantle (Anderson and Jordan, 1970). This chemical layering would create a barrier to vertical motion across the layer boundary and would inhibit mantle-wide convection. The existence of the chemical layering has been questioned in other studies using velocity-density systematics which suggest that the mantle is homogeneous with respect to iron content (Watt et al., 1975). Nonetheless, it is of interest to see how adding the constraint of no vertical flow across the boundary between the upper and lower mantle affects the flow.

To investigate this effect, we computed the flow for the "Cathles" model with vertical flow prohibited across the 700 km depth. The horizontal velocity and shear stress were constrained to be continuous across the boundary and the vertical velocity set equal to zero. The normal stress is discontinuous. The change in normal stress across the boundary can be interpreted physically as the stress induced by buoyancy forces caused by the displacement of the layer boundary by the flow.

The direction of the velocity vectors for this model is quite similar to those for the "rigid" model. The sections are not shown because of space limitations. The chief difference is that at depths of greater than about 350 km, the velocities have greater magnitude in the model which permits horizontal, but no vertical, flow at 700 km. For this model, the correlation coefficient r is 0.34, significant at a confidence level of only 82%.

DISCUSSION

It is remarkable that the correlation between the flow dips and the observed dips of the Benioff zones is so good for those models which allow whole mantle flow. Some caution is needed, however, in attaching significance to this correlation.

First, the flow models are time-independent. Since the energy equation has been ignored in these models and the Stokes equation is independent of time for low Reynolds number flow, the only time dependence in these models would enter through the time dependence of the boundary conditions. The models that are shown give the instantaneous velocity vectors for the present-day distribution of ridges and trenches. Since there is relative motion between the ridges and trenches, the velocity vector at a fixed point will change slowly with time. Thus the velocity vectors plotted are not particle trajectories.

This time dependence of the boundary conditions should have two effects on the dip angle. First, the change in the configuration of ridges and trenches will change the large scale flow driven by the moving plates. However, insofar as the rate of relative motion between ridges and trenches is small compared to the velocities of the subducted plates, the rearrangement of the large-scale flow pattern will take place on a time scale that is long in relation to the time it takes a subducted slab to sink through the upper mantle. Thus, neglecting the change in the large-scale flow pattern due to the relative motion of ridges and trenches should have only a minor effect on the subduction zone dips given by our models. The local flow in the region of a subduction zone should not change greatly due to the relative motion of a far away ridge during the time that a subducted slab can be identified by its seismic activity.

The second, more important, effect on the dip of a subducted slab which is not included in these time-independent models arises from the migration of the point of subduction. Even if each point of a subducted slab were sinking vertically, the dip of the slab would not be vertical if the location of the trench moved sufficiently rapidly.

Although it is not easy to determine the magnitude of this effect without making time-dependent models, we can set an upper bound on its magnitude. If a plate is being subducted with velocity v_s, a point on the slab travels a vertical distance $v_s \sin \theta$ and horizontal distance $v_s \cos \theta$ per unit time, where θ is the dip angle of the flow. If during this time the overriding slab is moving with velocity v_0, the trench will be displaced a distance v_0 over the subducted slab. If no change in flow pattern occurs during this time, the dip of the slab will be:

$$\theta_c = \tan^{-1} \frac{\sin \theta}{\frac{v_0}{v_s} + \cos \theta}$$

This is an upper bound to the effect of the moving trench on the dip of the

slab, since the instantaneous flow driven by the plates will always be in a sense to reduce the change in dip induced by the trench motion.

To assess the importance of this effect, it is necessary to compare the relative magnitudes of the velocities of the overriding plate and the subducted plate. Examination of Fig. 2 shows that, in the absolute frame of reference used, the overriding plate is moving much slower than the subducted plate in a direction perpendicular to the trench for most subduction zones.

The values of v_0, v_s, θ, θ_c and θ_s, the seismic dip of the subduction zone, are given for each of the ten subduction zones in Table I. For most of the subduction zones, the upper bound to the change in dip caused by trench motion is not large. The correlations between flow dip and seismic dip are not changed significantly if the "corrected" dip angles are used. For the "constant" model, $r = 0.83$; for the "Cathles" model, $r = 0.89$, and for the "rigid" model, $r = 0.15$.

A second inadequacy of the models is that they do not include the density contrast of the downgoing slab. Since the slab is denser than the surrounding mantle, it would be expected to descend at a steeper angle than that predicted by the simple flow model. Including this effect should shift all of the flow dips closer to 90° (vertical), decreasing the slope of the regression line, but not affecting the correlation significantly. Work is in progress to determine the magnitude of this effect. However, it is difficult to see how it could substantially affect the correlation coefficient.

A third limitation of the models is that, since the viscosity distribution is radially symmetric, the effect of the higher viscosity of the slab is not included. As a result, the flow in the models resulting from the mass flux of the lithosphere itself does not form a concentrated plume moving at the speed of the subducted slab, but is accommodated by a slower, more diffuse downwelling. As a result, less vorticity is generated in the models at the "corner" between the surface and the subducted material. The effect of this vorticity would be to oppose the bending of the lithosphere around this corner. Thus, flow models omitting the high viscosity slab should predict steeper dips than those which include the slab. It is very difficult to assess the magnitude of this effect.

The three oversimplifications in the model just discussed work in opposite directions. Ignoring the trench motion and the high viscosity of the slab tend to make the dips predicted by the model too steep. These effects may have been partly cancelled by the neglect of the density contrast in the slab, which tends to make the model slab dip too shallow. The significance of the correlation between seismic dip and flow dip for the two models which allow flow in the lower mantle and the nearness of the slope of the regression line to unity suggest that the net effect of these simplifying assumptions is small.

CONCLUSIONS

Although the models developed here are kinematic, neglecting the buoyancy forces which must drive the plates, they incorporate the observed com-

plex plate geometries and velocities as boundary conditions. They thus make it possible to isolate and understand the large scale flow due to the mass flux and viscous drag of the moving plates. Insofar as the large scale flow is dominated by the motions of the boundaries, these models should give a good representation of this flow. Small-scale thermal convection may be superimposed on this large scale flow.

For those models in which the viscosity structure and lack of chemical stratification permit flow to penetrate deeper than 700 km, the dips of the velocity vectors in the flow models match the dips of the Benioff zones remarkably well. The correlation between the flow dip and the seismic dip is statistically significant to better than the 99% confidence level.

We interpret this correlation to mean that the dips of subducted slabs are determined primarily by the large scale flow imposed by the plates moving in their observed geometry. The presence of the slabs does not change the flow direction significantly, and although the slabs may be important in the dynamics of mantle flow, they are oriented as if they were responding passively to the flow driven by the surface motion of the plates. This interpretation rules out convection confined to the upper mantle.

That the interactive global flow is important requires caution in local models of subduction zones. A thick boundary layer accompanies the moving plate in those models which successfully predict the dips of subducted slabs. This boundary layer may be important in the thermal evolution of slabs.

In areas of convergence in which both converging plates have similar crustal types it appears that the global flow determines which plate is underthrust. Examples include the Himalayas, the New Hebrides region, and the Tonga region. Thus geologic models in which the sense of subduction suddenly change (Dewey and Bird, 1970) seem to be unfeasible.

ACKNOWLEDGEMENTS

Sean Solomon kindly provided digitized plate boundary data and relative poles of rotation. Hager was supported by a National Science Foundation Graduate Fellowship for part of the time occupied by this research. This research was also supported by the National Science Foundation, grant EAR 75-22433.

APPENDIX

The equations of motion for a Newtonian fluid are transformed from second order differential equations into a set of coupled first order equations. This transformation is similar to the transformation of the second order equations describing the earth's elastic oscillations outlined by Alterman et al. (1959). The equations of motion of a Newtonian fluid are identical to those of an elastic body at zero frequency if strain rate and viscosities are substituted for strain and elastic moduli in the elastic equations. The derivation of the viscous equations is outlined on next pages.

The flow velocity and stress are expressed in terms of vector spherical harmonics as:

$$v_r = y_1^{lm} Y^{lm}$$

$$v_\theta = y_2^{lm} Y_\theta^{lm} + y_5^{lm} Y_\phi^{lm}$$

$$v_\phi = y_2^{lm} Y_\phi^{lm} - y_5^{lm} Y_\theta^{lm}$$

$$\tau_{rr} = y_3^{lm} Y^{lm}$$

$$\tau_{r\theta} = y_4^{lm} Y_\theta^{lm} + y_6^{lm} Y_\phi^{lm}$$

$$\tau_{r\phi} = y_4^{lm} Y_\phi^{lm} - y_6^{lm} Y_\theta^{lm}$$

In these equations, v_r, v_θ, and v_ϕ are the components of velocity in the radial, southerly, and easterly directions. The deviatoric normal stress in the radial direction is τ_{rr}. The components of radial shear in the southerly and easterly directions are $\tau_{r\theta}$ and $\tau_{r\phi}$. Y^{lm} are the surface spherical harmonics of degree l and order m normalized such that their root mean square is unity. θ and ϕ are colatitude and longitude.

$$Y^{lm} = P^{lm}(\cos\theta) \begin{bmatrix} \cos m\phi \\ \sin m\phi \end{bmatrix}$$

Also:

$$Y_\theta^{lm} \equiv \frac{\partial}{\partial\theta}(P^{lm})$$

and:

$$Y_\phi^{lm} \equiv \frac{1}{\sin\theta}\frac{\partial}{\partial\phi}(P^{lm})$$

The y_i^{lm} are functions of radius. Summation over the repeated superscripts l and m is implicit.

Both poloidal (spheroidal) and toroidal fields are necessary to describe an arbitrary displacement pattern. Coefficients y_1^{lm} through y_4^{lm} are associated with poloidal fields; y_5^{lm} and y_6^{lm} are associated with toroidal fields.

For incompressible flow with no vertical displacement of the boundaries, there is no perturbation of the gravity field. The Stokes equations can be transformed into the coupled first order differential equations:

$$\dot{y}_1^{lm} = -2y_1^{lm}/r + Ly_2^{lm}/r \tag{1}$$

$$\dot{y}_2^{lm} = -y_1^{lm}/r + y_2^{lm}/r + y_4^{lm}/\eta \tag{2}$$

$$\dot{y}_3^{lm} = 12\eta y_1^{lm}/r^2 - 6L\eta y_2^{lm}/r^2 + Ly_4^{lm}/r \tag{3}$$

$$\dot{y}_4^{lm} = -6\eta y_1^{lm}/r^2 + 2\eta(2L-1)y_2^{lm}/r^2 - y_3^{lm}/r - 3y_4^{lm}/r^2 \tag{4}$$

$$\dot{y}_5^{lm} = y_5^{lm}/r + y_6^{lm}/\eta \tag{5}$$

$$\dot{y}_6^{lm} = (L-2)\eta y_5^{lm}/r^2 - 3y_6^{lm}/r \tag{6}$$

Here $\dot{y}_i$ is dy_i/dr, $L = l(l+1)$ and η is the viscosity. The poloidal and toroidal equations are decoupled.

Similar reductions of the second order differential equations of motion to sets of coupled first order differential equations have been carried out for viscous flow by Takeuchi and Hasegawa (1965) and Kaula (1975), and for elastic oscillations by Alterman et al. (1959). Takeuchi and Hasegawa (1965) derived the poloidal equations, but some of the coefficients are misprinted in their paper. Kaula (1975) derived both the poloidal and the torroidal equations, but his torroidal equations contain a misprint. Equations 1—4 agree with the poloidal equations of Kaula (1975) and equations 1—6 agree with the equations of Alterman et al. (1959) for zero frequency and infinite Lame parameter λ, corresponding to incompressible flow.

These two coupled sets of equations could be solved numerically. However, with the change in variables:

$$u_1 = y_1$$

$$u_2 = y_2$$

$$u_3 = ry_3/\eta$$

$$u_4 = ry_4/\eta$$

$$v_1 = y_5$$

$$v_2 = ry_6/\eta$$

$$\lambda = \ln(r/a)$$

with a the radius of the earth, the sets of equations become

$$\frac{du^{lm}}{d\lambda} = A^l u^{lm} \tag{7}$$

$$\frac{dv^{lm}}{d\lambda} = B^l v^{lm} \,. \tag{8}$$

Here:

$$A^l = \begin{bmatrix} -2 & L & 0 & 0 \\ -1 & 1 & 0 & \eta^* \\ 2\eta^* & -6L\eta^* & 1 & L \\ -6\eta^* & 2(2L-1)\eta^* & -1 & -2 \end{bmatrix}$$

and:

$$B^l = \begin{bmatrix} 1 & 1/\eta^* \\ (L-2)\eta^* & -2 \end{bmatrix}$$

where $\eta^* = \eta/\eta_0$, and η_0 is a reference viscosity.

Equations 7 and 8 are homogeneous differential equations which can be solved analytically by the propagator matrix technique (Gantmacher, 1960; Gilbert and Backus, 1966; Cathles, 1975). The solution to eq. 7 for a layer in which A is constant is:

$$u^{lm}(\lambda) = \exp[(\lambda - \lambda_0)A^l u^{lm}(\lambda_0)] = P^l(\lambda, \lambda_0)u^{lm}(\lambda_0)$$

where $P^l(\lambda, \lambda_0)$ is the propagator matrix which propagates the vector u^{lm} from λ_0 to λ.

Boundary conditions

At the surface of the earth, the radial velocity is constrained to be zero and the observed horizontal plate motions are imposed. The core—mantle boundary is taken to be free slip. Then, at the core—mantle boundary:

$$u^{lm}_{r=c} = [0, u^{lm}_{2c}, u^{lm}_{3c}, 0]^T$$

and:

$$v^{lm}_{r=c} = [v^{lm}_{1c}, 0]^T$$

At the surface, $r = a$:

$$u^{lm}_{r=a} = [0, u^{lm}_{2a}, u^{lm}_{3a}, u^{lm}_{4a}]^T$$

and:

$$v^{lm}_{r=a} = [v^{lm}_{1a}, v^{lm}_{2a}]^T$$

Since u^{lm}_{2a} and v^{lm}_{1a} are the known coefficients in the spheroidal and toroidal expansions of the plate velocities of degree l and order m, the constraint that:

$$u^{lm}_a = P^l(\lambda a, \lambda c)u^{lm}_c$$

and similarly for v^{lm} leads to two sets of simultaneous equations which are solved for u^{lm}_c and v^{lm}_c. Then u^{lm} and v^{lm} can be determined at any radius by propagating these starting vectors upward.

REFERENCES

Alterman, Z.H., Jarosch, H. and Pekeris, C.L., 1959. Oscillations of the earth. Proc. R. Soc. London, Ser. A, 252: 80—95.

Anderson, D.L. and Jordan, T.M., 1970. The composition of the lower mantle. Phys. Earth Planet. Inter., 3: 23.

Anderson, R.N., 1975. Heat flow in the Mariana marginal basin. J. Geophys. Res., 80: 4043—4048.

Ansell, J.H. and Smith, E.G.C., 1975. Detailed structure of a mantle seismic zone using the homogeneous station method. Nature, 253: 518—520.

Ashby, M.F. and Verrall, R.A., 1977. Micromechanisms of flow and fracture, and their

relevance of the rheology of the mantle. Philos. Trans. R. Soc. London, Ser. A, 288: 59—95.
Barazangi, M. and Isacks, B.L., 1976. Spatial distributions of earthquakes and subduction of the Nazca plate beneath South America. Geology, 4: 686—692.
Cathles, L.M. III, 1975. The Viscosity of the Earth's Mantle. Princeton University Press, Princeton, N.J., 386 pp.
Chandrasekhar, S., 1961. Hydrodynamic and Hydromagnetic Stability. University Press, Oxford, 654 pp.
Cohn, S.N., 1975. Distribution of Earthquakes in the Tonga—Kermadec and Izu—Bonin—Japan—Kuril—Kamchatka Trench Systems. Thesis, Harvard College, Cambridge (unpublished).
Cramer, H., 1946. Mathematical Methods of Statistics. Princeton University Press, Princeton, N.J.
Davies, G.F., 1977. Viscous mantle flow under moving lithospheric plates and under subduction zones. Geophys. J. R. Astron. Soc., 49: 557—563.
Dewey, J.W. and Algermissen, S.T., 1974. Seismicity of the Middle America arc-trench system near Managua, Nicaragua. Bull. Seismol. Soc. Am., 64: 1033—1048.
Dewey, J.F. and Bird, F.M., 1970. Mountain belts and the new global tectonics. J. Geophys. Res., 75: 2625—2647.
Engdahl, E.R., 1973. Relocation of intermediate depth earthquakes in the central Aleutians by seismic ray tracing. Nature, Phys. Sci., 245: 23—25.
Fitch, T.J., 1972. Plate convergence, transcurrent faults and internal deformation adjacent to Southeast Asia and the Western Pacific. J. Geophys. Res., 77: 4432—4460.
Fitch, T.J. and Molnar, P., 1970. Focal mechanisms along inclined earthquake zones in the Indonesian—Philippine region. J. Geophys. Res., 75: 1431—1444.
Forsyth, D. and Uyeda, S., 1975. On the relative importance of the driving forces of plate motion. Geophys. J. R. Astron. Soc., 43: 163—200.
Gantmacher, F.R., 1960. The Theory of Matrices. Vols. 1 and 2. Chelsea Publishing Co., New York. (Translated from Russian by K.A. Hirsch.)
Gaposhkin, E.M., 1974. Earth's gravity field to the eighteenth degree and geocentric coordinates for 104 stations from satellite and terrestrial data. J. Geophys. Res., 79: 5377—5411.
Gaposhkin, E.M. and Lambeck, K., 1970. 1969 Smithsonian standard Earth (2). Spec. Rep., 315, Smithsonian Astrophysical Observ., Cambridge, Mass., 93 pp.
Gilbert, F. and Backus, G.E., 1966. Propagator matrices in elastic wave and vibration problems. Geophysics, 31: 326—332.
Hager, B.H. and O'Connell, R.J., 1978. Kinematic models of large scale flow in the earth's mantle. J. Geophys. Res., in press.
Isacks, B.L. and Barazangi, M., 1977. Geometry of Benioff zones: lateral segmentation and downwards bending of the subducted lithosphere. In: M. Talwani and W.C. Pitman, III (Editors), Island Arcs, Deep Sea Trenches, and Back-Arc Basins. American Geophysical Union, Washington, D.C., 480 pp.
Isacks, B. and Molnar, P., 1971. Distribution of stresses in the descending lithosphere from a global survey of focal-mechanism solutions of mantle earthquakes. Rev. Geophys. Space Phys., 9: 103—174.
Karig, D.E., 1971. Structural history of the Mariana Island arc system. Geol. Soc. Am. Bull., 82: 323—344.
Kaula, W.M., 1975. Product-sum conversion of spherical harmonics with application to thermal convection. J. Geophys. Res., 80: 225—231.
McKenzie, D. and Weiss, N., 1975. Speculations on the thermal and tectonic history of the earth. Geophys. J.R. Astron. Soc., 42: 131—174.
Minster, J.B., Jordan, T.H., Molnar, P. and Haines, E., 1974. Numerical modeling of instantaneous plate tectonics. Geophys. J. R. Astron. Soc., 36: 541—576.
O'Connell, R.J., 1977. On the scale of mantle convection. Tectonophysics, 38: 119—136.

Parmentier, E.M. and Turcotte, D.L., 1976. Studies of thermal convection beneath a rigid lithosphere. EOS, Trans. Am. Geophys. Union, 57: 329.

Parmentier, E.M., Turcotte, D.L. and Torrance, K.E., 1976. Studies of finite amplitude non-Newtonian thermal convection with application to convection in the earth's mantle. J. Geophys. Res., 81: 1839—1846.

Peltier, W.R. and Andrews, J.T., 1976. Glacial-isostatic adjustment — I. The forward problem. Geophys. J. R. Astron. Soc., 46: 605—646.

Richardson, R.M., Solomon, S.C. and Sleep, N.H., 1976. Intraplate stress as an indicator of plate tectonic driving forces. J. Geophys. Res., 81: 1847—1856.

Richter, F.M., 1973. Dynamical models for sea floor spreading. Rev. Geophys. Space Phys., 11: 223—287.

Richter, F.M. and Parsons, B., 1975. On the interactions of two scales of convection in the mantle. J. Geophys. Res., 80: 2529—2541.

Solomon, S.C., Sleep, N.H. and Richardson, R.M., 1975. On the forces driving plate tectonics: inferences from absolute plate velocities and intraplate stress. Geophys. J. R. Astron. Soc., 42: 769—801.

Takeuchi, H. and Hasegawa, Y., 1965. Viscosity distribution in the earth. Geophys. J. R. Astron. Soc., 9: 503—508.

Wagner, C.A., Lerch, F.J., Brownd, J.E. and Richardson, J.A., 1977. Improvement in the geopotential derived from satellite and surface data (GEM 7 and 8). J. Geophys. Res., 82: 901—913.

Walcott, R.J., 1973. Structure of the earth from glacio-isostatic rebound. In: F.A. Donath (Editor), Annual Reviews of Earth and Planetary Sciences. Annual Reviews, Inc., Palo Alto, Calif., pp. 15—37.

Watt, J.P., Shankland, T.J. and Mao, N., 1975. Uniformity of mantle composition. Geology, 3: 91—94.